Supporting Information (SI) for:

# Ground-State $pK_a$ and Physicochemical Characterization of Resveratrone as a pH-Responsive Organic Fluorophore

*Myeong Jin Kim,*[a] *Jong Woo Lee*[a*]

[a] Department of Applied Chemistry, College of Natural Science, University of Seoul, Seoul, 02504, Republic of Korea

**Determination of the Linear dynamic range (LDR) and limit of detection (LOD)**

The fluorescence response of resveratrone as a function of pH follows a sigmoidal calibration curve, as is characteristic of indicator-based optical pH sensors.[1] According to the IUPAC definition, the LDR is defined as the concentration interval over which the analytical signal is directly proportional to the analyte concentration. Within such a sigmoidal response, the maximum analytical sensitivity — defined by IUPAC as the slope of the signal-versus-analyte-concentration plot ($\Delta S/\Delta pH$) — is obtained near the inflection point (i.e., near the $pK_a$), where the response is approximately linear.[1] Beyond ±1.5 pH units from this inflection point, the slope approaches zero and the sensor response becomes nonlinear.[1]

The LDR was therefore determined by applying least-squares linear regression to successive subsets of the sigmoidal calibration data. The pH interval yielding a coefficient of determination of $R^2 \geq 0.99$ was identified as the LDR, as $R^2$ is widely used as a standard indicator of linearity in analytical calibration, with $R^2 \geq 0.99$ representing an accepted threshold for reliable linear response.[2] The slope (k) of the linear regression within the LDR was taken as the analytical sensitivity of the sensor for each experimental condition.[1,2]

The resulting LDR values were pH 7.12–8.96 (k = 16411.6 a.u. $pH^{-1}$, $R^2$ = 0.991) in the presence of BSA, and pH 6.83–8.68 (k = 11955.0 a.u. $pH^{-1}$, $R^2$ = 0.993) in the presence of metal ions ($Mg^{2+}$ and $Ca^{2+}$).

The limit of detection was calculated according to the IUPAC-recommended formula:[3]

$$LOD = \frac{3\sigma}{k}$$

where σ is the standard deviation of the blank signal and k is the slope (analytical sensitivity) of the linear regression within the LDR.

Specifically, σ was determined as the standard deviation of ten replicate fluorescence measurements (area under the emission curve) recorded at the highest pH within the respective LDR where the fluorescence intensity is at its minimum within the linear range. This approach reflects the instrumental and spectroscopic noise under the most signal-limited experimental conditions within the LDR, rather than the residual standard deviation of the linear fit.[3] The LOD was calculated to be 0.14 pH units under both the BSA and metal ion conditions, with the identical values reflecting the proportionally different σ and k across the two experimental matrices rather than a methodological inconsistency.

**Supplementary references**


(1) A. Steinegger, O. S. Wolfbeis and S. M. Borisov, *Chem. Rev.*, 2020, **120**, 12357–12489.
(2) J. N. Miller and J. C. Miller, *Statistics and Chemometrics for Analytical Chemistry*, Pearson Education, Harlow, **7th edn**, 2018.
(3) G. L. Long and J. D. Winefordner, *Anal. Chem.*, 1983, **55**, 712A–724A.

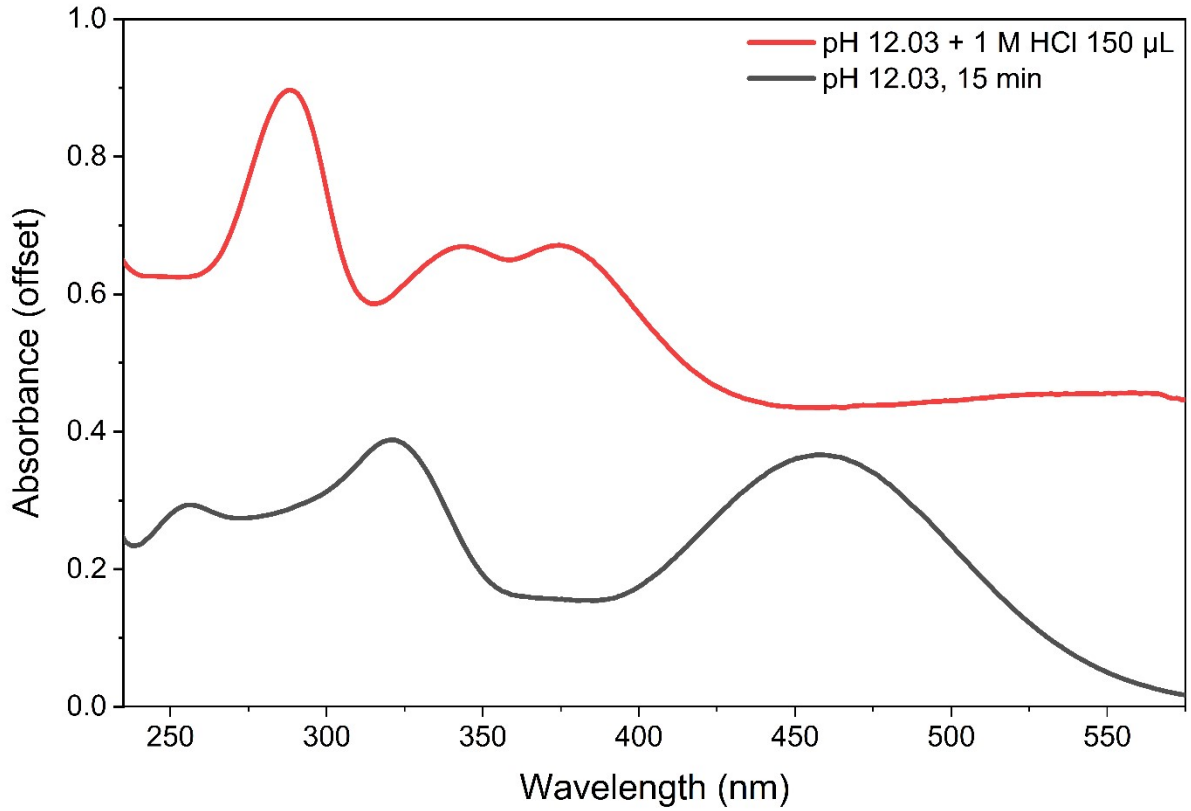


**Fig. S1** Reversible spectral change of resveratrone at pH 12.03. The absorption spectrum was recorded 15 min after solution preparation (gray), followed by addition of 1 M HCl (150 µL) (red).

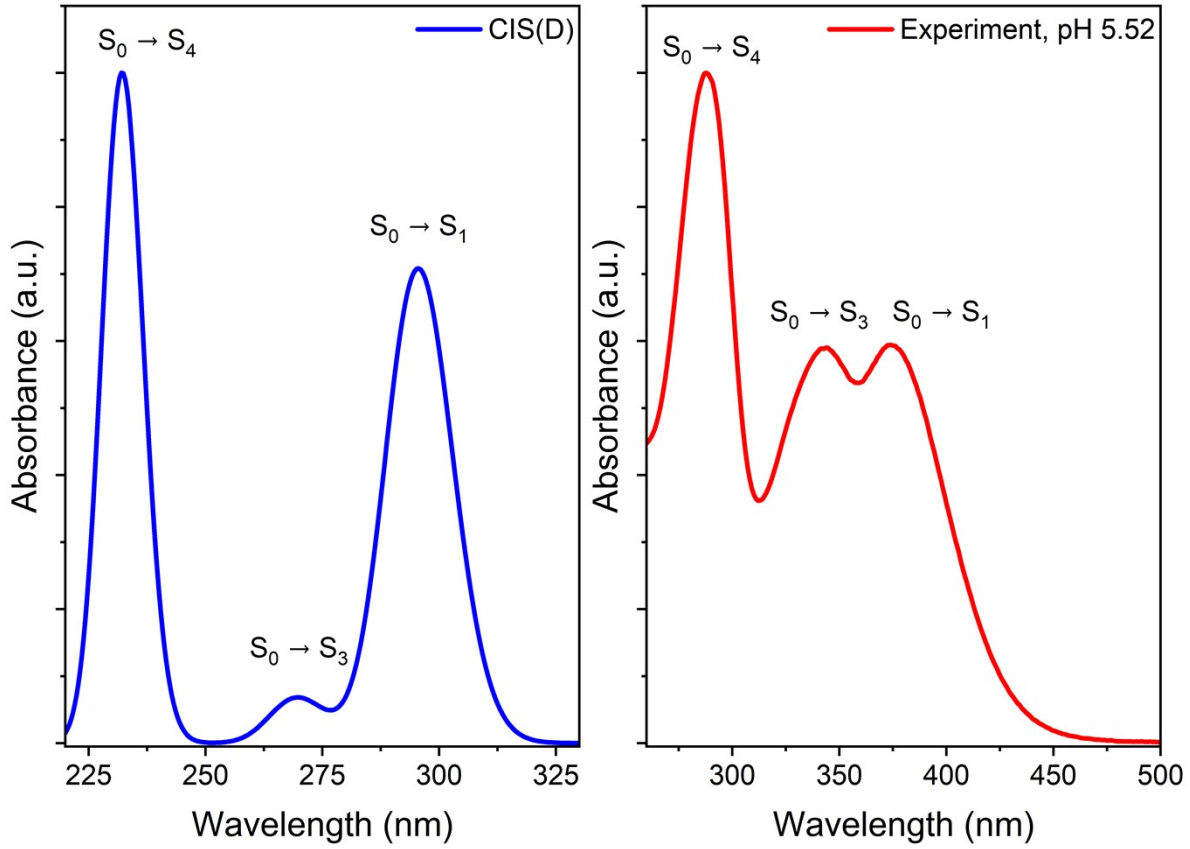


**Fig. S2** Comparison of experimental and simulated absorption spectra of the neutral species. While all vertical excitation energies reported in the main text and Tables S1–S4 (covering the neutral, monoanionic, and dianionic forms) were computed at the CAM-B3LYP/6-311++G(d,p)//B3LYP/6-311++G(d,p) level to ensure methodological consistency and quantitative accuracy across all protonation states, the simulation shown here was performed at the CIS(D)/def2-TZVP//B3LYP/6-311++G(d,p) level, which was selected specifically for its ability to reproduce the qualitative spectral envelope of the neutral ground-state absorption. Notably, both levels of theory consistently predict that the $S_0 \rightarrow S_2$ transition carries negligibly small oscillator strength and is therefore absent from the simulated spectrum, in agreement with the results in Table S1. This concordance across distinct theoretical frameworks confirms the robustness of the assignment and reflects a consistent trend throughout all employed computational methodologies.

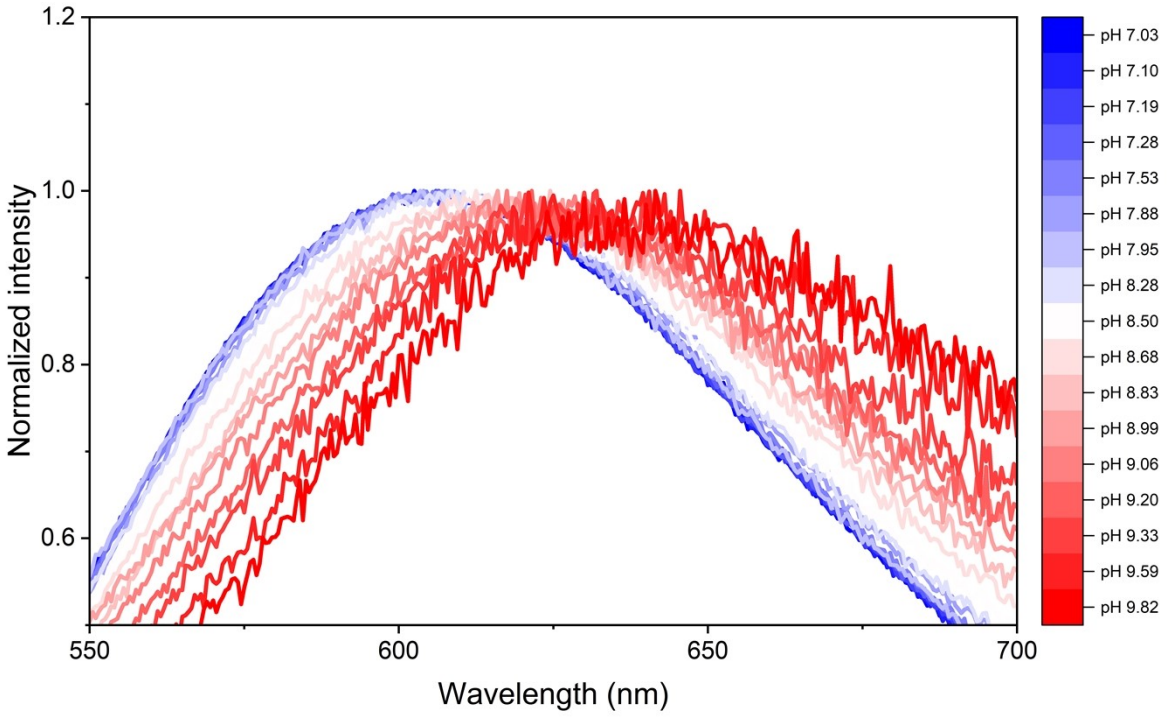


**Fig. S3** Normalized photoluminescence spectra of resveratrone (λex = 376 nm) exhibit a peak shift with increasing pH.

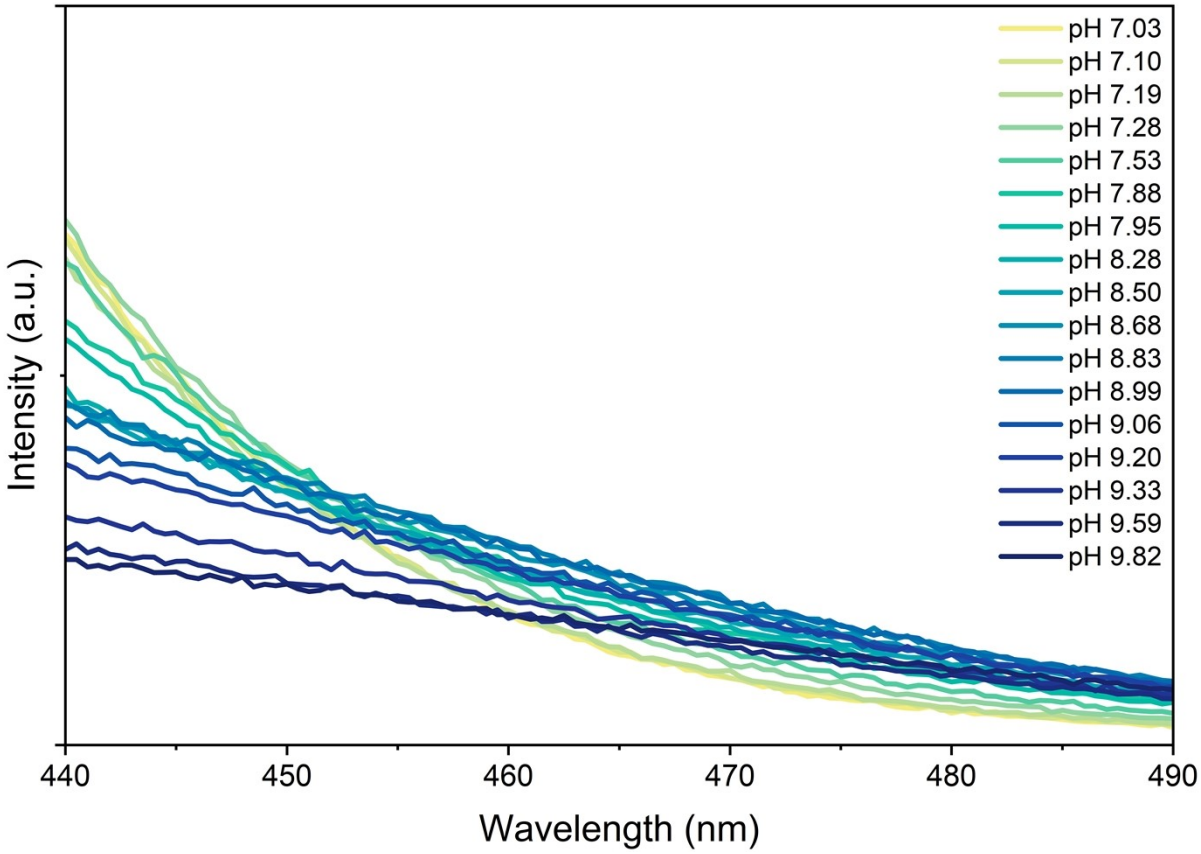


**Fig. S4** Expanded view of Figure 5b in the 450–490 nm region.

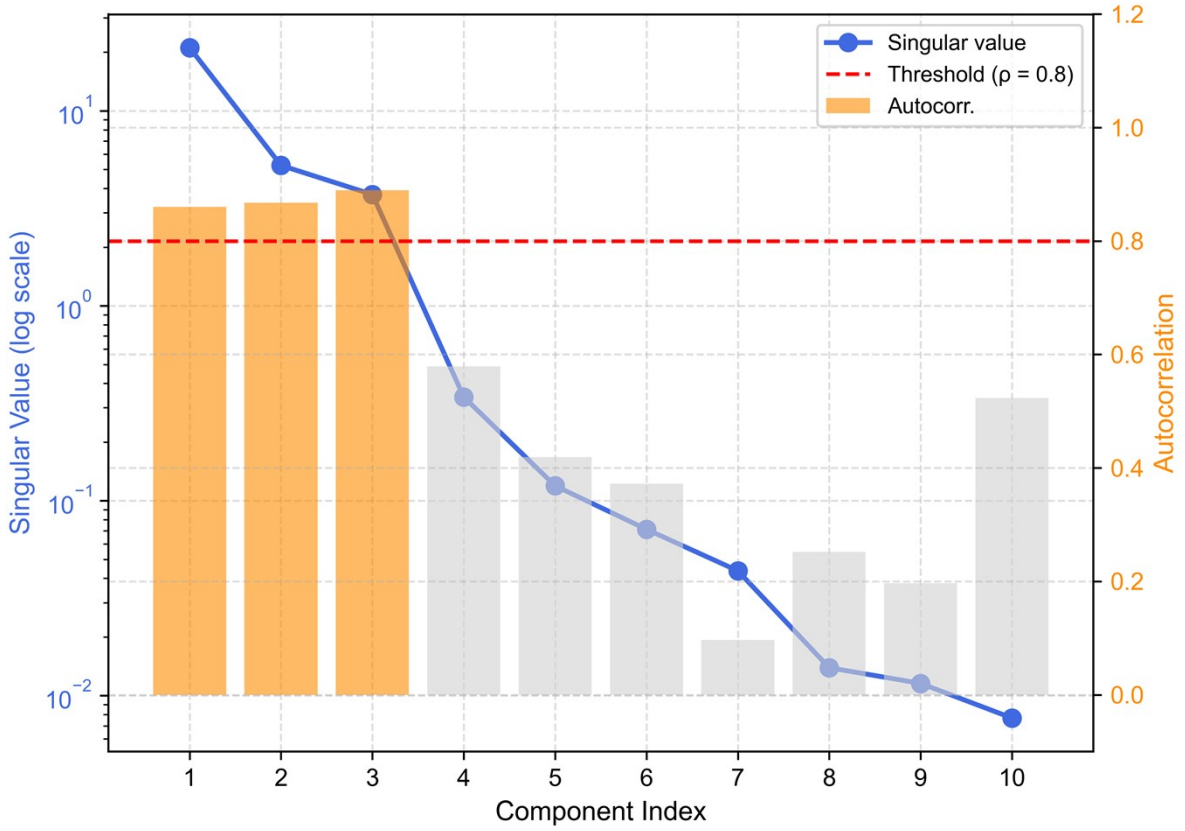


**Fig. S5** Scree plot and autocorrelation analysis for SVD of the pH-dependent absorption spectra of resveratrone. Blue circles connected by a line represent the singular values plotted on a logarithmic scale (left axis). Orange bars indicate the autocorrelation values (ρ) of the corresponding right singular vectors (right axis). The red dashed line denotes the threshold of ρ = 0.8, above which components are considered significant. The first three components satisfy this criterion and were retained for subsequent analysis.

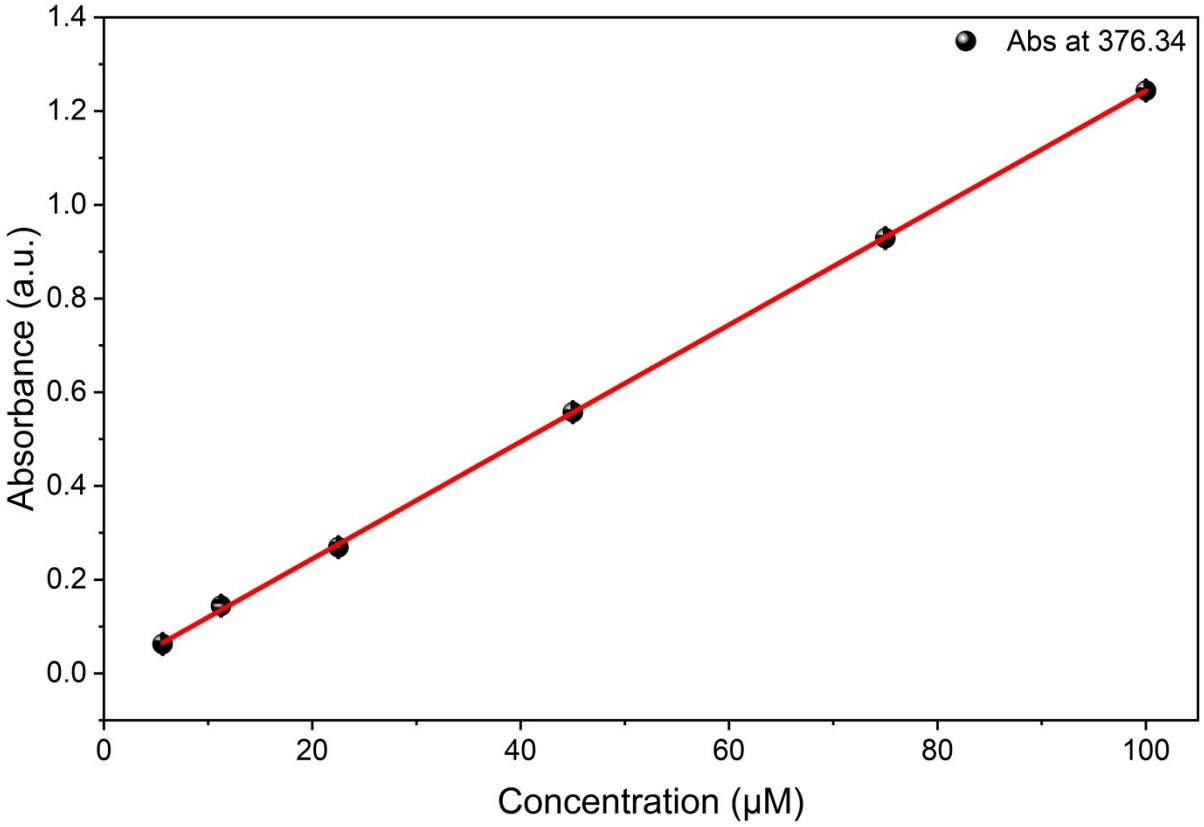


**Fig. S6** Beer–Lambert linearity of resveratrone in aqueous solution at 376 nm. The red line represents a linear fit to the experimental data.

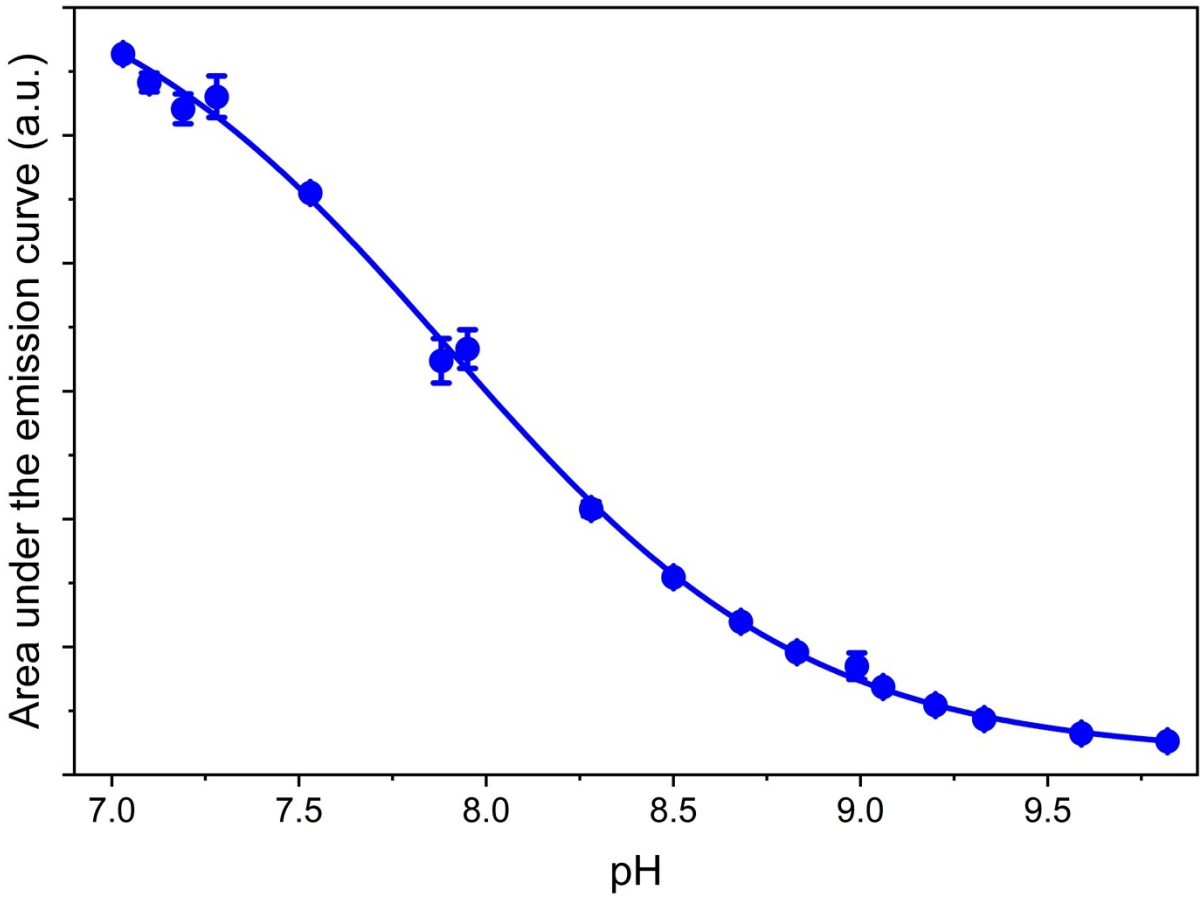


**Fig. S7** Integrated fluorescence emission intensity of 20 μM resveratrone as a function of pH ($\lambda_{ex}$ = 376 nm). The value of the inflection point is 7.88.

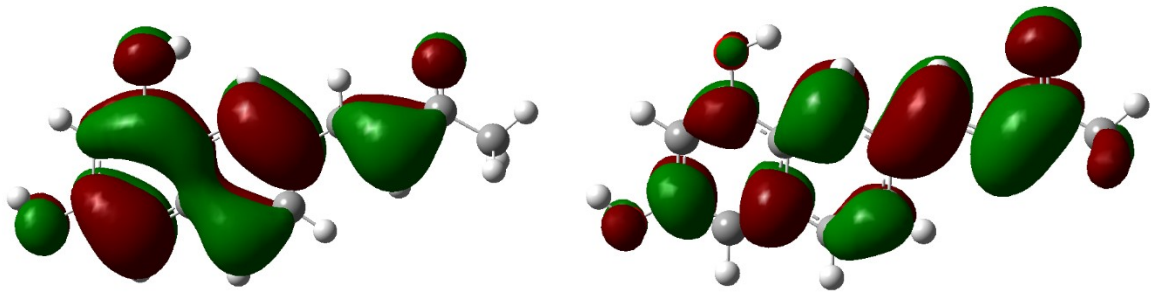

**Fig. S8** Natural transition orbital analysis for the S1 excited state of the molecular form of resveratrone. The highest occupied transition orbital (HOTO, left) and the lowest unoccupied transition orbital (LUTO, right) represent the dominant NTO pair with an eigenvalue of $\lambda$ = 0.955, accounting for 95.5% of the S1 transition. The HOTO exhibits a delocalized $\pi$ bonding character over the hydroxyl-substituted aromatic ring and the vinyl bridge, while the LUTO displays $\pi^*$ antibonding character extending toward the carbonyl fragment, indicating an intramolecular charge transfer (ICT) nature of the S1 transition. Isosurfaces are plotted at an isovalue of ±0.02 a.u.

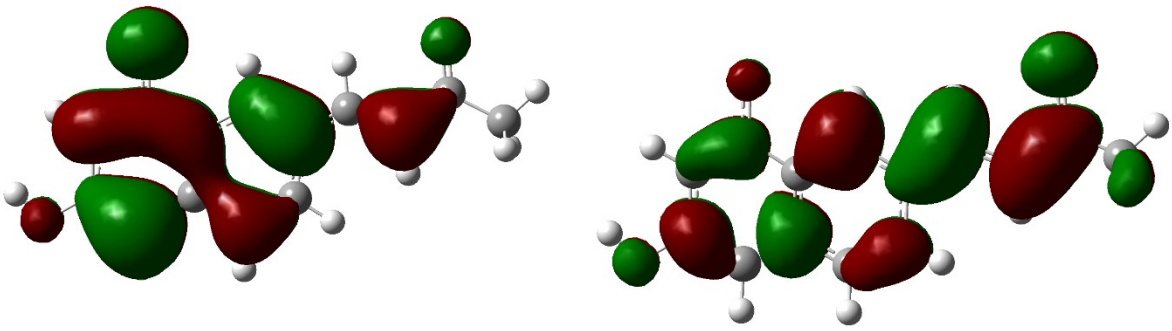

**Fig. S9** Natural transition orbital analysis for the S1 excited state of the 1-anion form of resveratrone. The highest occupied transition orbital (HOTO, left) and the lowest unoccupied transition orbital (LUTO, right) represent the dominant NTO pair with an eigenvalue of $\lambda$ = 0.967, accounting for 96.7% of the S1 transition. Isosurfaces are plotted at an isovalue of ±0.02 a.u.

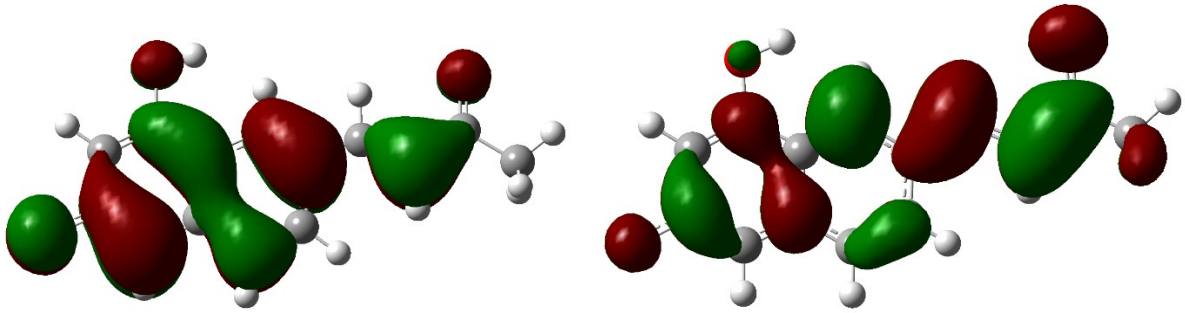

**Fig. S10** Natural transition orbitals (NTOs) for the S1 excited state of the 3-anion form of resveratrone. The highest occupied transition orbital (HOTO, bottom) and the lowest unoccupied transition orbital (LUTO, top) represent the hole and particle orbitals, respectively. The NTO eigenvalue of the dominant pair is $\lambda = 0.968$, indicating that the S1 transition is essentially described by a single NTO pair (96.8% contribution). Isosurfaces are plotted at an isovalue of ±0.02 a.u.

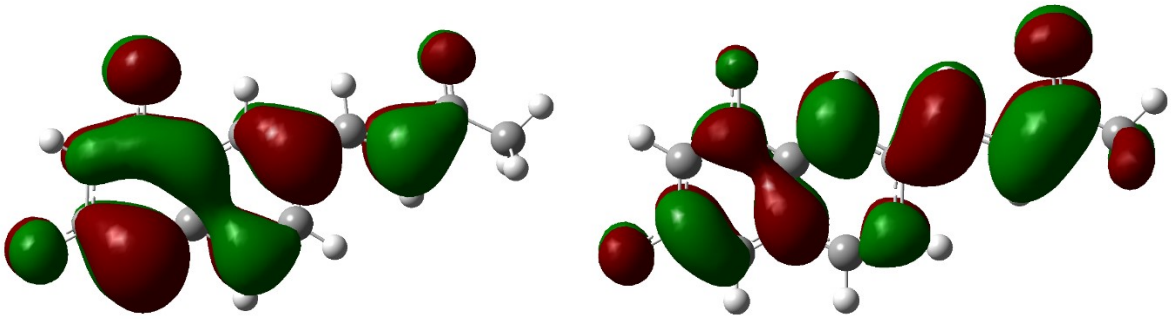

**Fig. S11** Natural transition orbitals (NTOs) for the S1 excited state of the dianion form of resveratrone. The highest occupied transition orbital (HOTO, bottom) and the lowest unoccupied transition orbital (LUTO, top) represent the hole and particle orbitals, respectively. The NTO eigenvalue of the dominant pair is $\lambda = 0.969$, indicating that the S1 transition is essentially described by a single NTO pair (96.9% contribution). Isosurfaces are plotted at an isovalue of ±0.02 a.u.

| Transition | λ (nm) | E (eV) | f | MO | Contribution (%) |
|---|---|---|---|---|---|
| $S_0 \rightarrow S_1$ | 336 | 3.69 | 0.8170 | HOMO-1 → LUMO+1<br>HOMO → LUMO | 2.79<br>91.89 |
| $S_0 \rightarrow S_2$ | 305 | 4.07 | 0.0001 | HOMO-3 → LUMO<br>HOMO-3 → LUMO+5 | 81.03<br>13.40 |
| $S_0 \rightarrow S_3$ | 300 | 4.14 | 0.0287 | HOMO → LUMO+1<br>HOMO-1 → LUMO<br>HOMO-1 → LUMO+5 | 65.97<br>23.55<br>2.67 |
| $S_0 \rightarrow S_4$ | 271 | 4.58 | 0.6319 | HOMO-1 → LUMO<br>HOMO → LUMO+1<br>HOMO-2 → LUMO<br>HOMO-1 → LUMO+1 | 58.08<br>26.75<br>4.52<br>4.26 |

**Table S1** Calculated vertical excitation energies, corresponding wavelengths, oscillator strengths (f), and dominant molecular orbital (MO) contributions for the excited states of the neutral (molecular) form obtained from TD-DFT calculations.

| Transition | λ (nm) | E (eV) | f | MO | Contribution (%) |
|---|---|---|---|---|---|
| $S_0 \rightarrow S_1$ | 398 | 3.11 | 0.7006 | HOMO → LUMO<br>HOMO → LUMO+6 | 92.00<br>2.63 |
| $S_0 \rightarrow S_2$ | 319 | 3.89 | 0.0787 | HOMO-3 → LUMO<br>HOMO-1 → LUMO<br>HOMO → LUMO+1 | 3.29<br>2.92<br>88.77 |
| $S_0 \rightarrow S_3$ | 300 | 4.13 | 0.0001 | HOMO-5 → LUMO<br>HOMO-5 → LUMO+6 | 83.17<br>10.84 |
| $S_0 \rightarrow S_4$ | 287 | 4.32 | 0.6042 | HOMO-4 → LUMO<br>HOMO-1 → LUMO<br>HOMO → LUMO+1<br>HOMO → LUMO+6 | 6.23<br>79.10<br>4.48<br>4.07 |

**Table S2** Calculated vertical excitation energies, corresponding wavelengths, oscillator strengths (f), and dominant molecular orbital (MO) contributions for the excited states of the 1-anion form obtained from TD-DFT calculations.

| Transition | λ (nm) | E (eV) | f | MO | Contribution (%) |
|---|---|---|---|---|---|
| $S_0 \rightarrow S_1$ | 385 | 3.22 | 1.0553 | HOMO → LUMO | 92.77 |
| $S_0 \rightarrow S_2$ | 331 | 3.75 | 0.0505 | HOMO-1 → LUMO<br>HOMO → LUMO+1 | 7.73<br>86.52 |
| $S_0 \rightarrow S_3$ | 300 | 4.13 | 0.0001 | HOMO-4 → LUMO<br>HOMO-4 → LUMO+6 | 83.44<br>9.61 |
| $S_0 \rightarrow S_4$ | 282 | 4.40 | 0.3212 | HOMO-3 → LUMO<br>HOMO-1 → LUMO<br>HOMO-1 → LUMO+1<br>HOMO → LUMO+1 | 7.73<br>71.77<br>4.90<br>8.52 |

**Table S3** Calculated vertical excitation energies, corresponding wavelengths, oscillator strengths (f), and dominant molecular orbital (MO) contributions for the excited states of the 3-anion form obtained from TD-DFT calculations.

| Transition | λ (nm) | E (eV) | f | MO | Contribution (%) |
|---|---|---|---|---|---|
| $S_0 \rightarrow S_1$ | 432 | 2.87 | 0.9510 | HOMO → LUMO | 93.26 |
| $S_0 \rightarrow S_2$ | 339 | 3.66 | 0.0288 | HOMO-1 → LUMO<br>HOMO → LUMO+2 | 9.28<br>84.51 |
| $S_0 \rightarrow S_3$ | 316 | 3.93 | 0.4387 | HOMO-3 → LUMO<br>HOMO-1 → LUMO<br>HOMO → LUMO+2 | 4.74<br>76.77<br>10.69 |
| $S_0 \rightarrow S_4$ | 295 | 4.20 | 0.0001 | HOMO-6 → LUMO<br>HOMO-6 → LUMO+6<br>HOMO-6 → LUMO+9 | 84.17<br>7.52<br>3.02 |

**Table S4** Calculated vertical excitation energies, corresponding wavelengths, oscillator strengths (f), and dominant molecular orbital (MO) contributions for the excited states of the dianion form obtained from TD-DFT calculations.

Resveratrone, optimized geometry in $S_0$ for spectrum prediction

B3LYP/6-311++G(d,p)

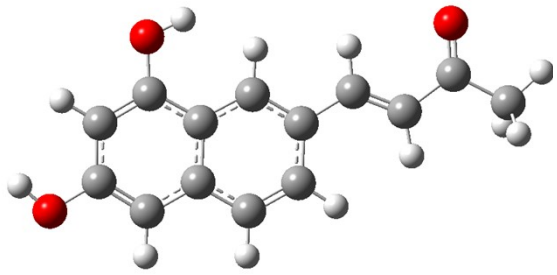

C -3.74706200 0.93207000 -0.00002500

C -2.43682200 1.35500000 -0.00000500

C -1.35879500 0.41495900 0.00000700

C -1.69464500 -0.98061800 0.00001200

C -3.04183600 -1.39499100 -0.00000300

C -4.04304700 -0.44571900 -0.00002400

H 0.28411200 1.83974800 -0.00001000

H -4.55008500 1.66094600 -0.00003400

C 0.00222000 0.79177900 0.00000900

C -0.62739300 -1.92687700 0.00003400

H -3.28852800 -2.44983600 0.00000200

C 0.68160500 -1.53158800 0.00004300

C 1.02756800 -0.14620600 0.00002600

H -0.87733700 -2.98224300 0.00004400

H 1.46260000 -2.28216700 0.00006100

O -2.23176500 2.71134400 0.00001700

O -5.34717100 -0.87815500 -0.00003500

H -1.29073400 2.92743300 0.00007400

H -5.94596000 -0.11869800 -0.00004000

C 2.40114500 0.32880700 0.00001800

C 3.52886300 -0.41532000 0.00000600

H 2.51611500 1.41039300 0.00002000

H 3.49516000 -1.49887400 0.00000300

C 4.86567400 0.19453900 -0.00001600

C 6.03199600 -0.75795000 -0.00005300

O 5.04431900 1.41906500 0.00000100

H 6.97624700 -0.21438500 -0.00019100

H 5.97934300 -1.40874200 0.87885300

H 5.97917300 -1.40892300 -0.87881200

Resveratrone 1-anion, optimized geometry in $S_0$ for spectrum prediction

CAM-B3LYP/6-311++G(d,p)

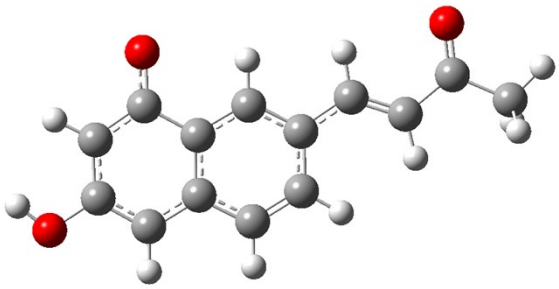

C 3.74170900 0.98034500 -0.00016100

C 2.41756500 1.44433200 -0.00020800

C 1.37197400 0.42654500 -0.00005500

C 1.71421400 -0.95560400 0.00011900

C 3.06172900 -1.35908600 0.00015100

C 4.03751000 -0.38495100 0.00000900

H -0.22571200 1.85127300 -0.00021300

H 4.55281300 1.70176500 -0.00026800

C 0.01919600 0.79551400 -0.00008300

C 0.65079400 -1.90470600 0.00025500

H 3.32880100 -2.40835100 0.00027800

C -0.65491500 -1.51575800 0.00022000

C -1.00423400 -0.13670800 0.00004800

H 0.90264900 -2.95967900 0.00038600

H -1.43294600 -2.26964300 0.00032500

O 2.12312800 2.69844000 -0.00038300

O 5.34904400 -0.80533300 0.00003800

H 5.93454400 -0.03781400 -0.00008100

C -2.37666900 0.33140300 -0.00000100

C -3.49835800 -0.41060800 0.00008400

H -2.49535500 1.41224000 -0.00012600

H -3.46660200 -1.49369000 0.00020500

C -4.82730100 0.20262300 0.00000900

C -5.99459000 -0.73919100 0.00009500

O -5.00061100 1.42257800 -0.00012300

H -6.93452200 -0.19010400 0.00005700

H -5.94395400 -1.38825200 -0.87824500

H -5.94394200 -1.38811400 0.87853600

Resveratrone 3-anion, optimized geometry in $S_0$ for spectrum prediction

CAM-B3LYP/6-311++G(d,p)

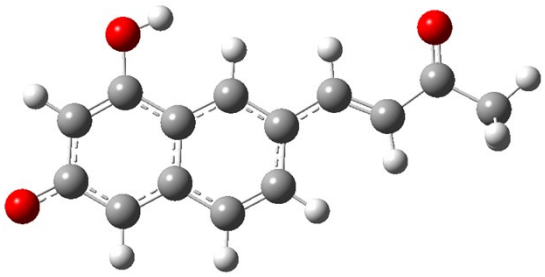

C -3.77822600 0.92136600 -0.00021200

C -2.48083100 1.33607400 -0.00014600

C -1.39805300 0.40292500 -0.00004900

C -1.74416400 -0.98490400 -0.00000800

C -3.08072300 -1.39598100 -0.00007200

C -4.13768100 -0.46964600 -0.00018200

H 0.23786400 1.82613000 -0.00004600

H -4.57110300 1.66103600 -0.00028500

C -0.04479100 0.77802500 -0.00000500

C -0.66998700 -1.92742400 0.00009500

H -3.31180400 -2.45587300 -0.00004000

C 0.63186900 -1.53407500 0.00013800

C 0.97932000 -0.15248400 0.00008400

H -0.91762800 -2.98326200 0.00013400

H 1.41316200 -2.28442500 0.00021300

O -2.25944400 2.69333400 -0.00019700

O -5.38355100 -0.81965900 -0.00024900

C 2.34867400 0.31902300 0.00010400

C 3.47348200 -0.41929600 0.00016300

H 2.46545400 1.40015700 0.00005900

H 3.44615900 -1.50244500 0.00020400

C 4.79876700 0.20023600 0.00016300

C 5.97116000 -0.73528600 0.00020300

O 4.96624200 1.42139800 0.00012800

H 6.90800200 -0.18091500 0.00023200

H 5.92431300 -1.38450600 0.87861800

H 5.92436900 -1.38450300 -0.87821700

H -1.31765800 2.89671800 0.00001600

Resveratrone dianion, optimized geometry in $S_0$ for spectrum prediction

CAM-B3LYP/6-311++G(d,p)

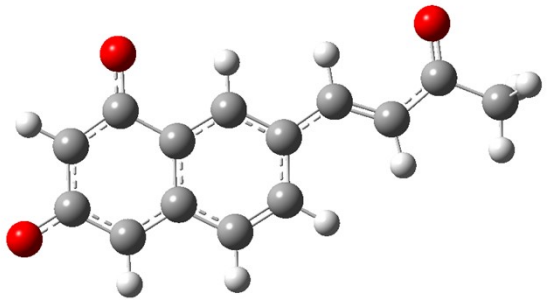

C -3.78666000 0.97392400 0.00005000

C -2.47073000 1.43442100 0.00003800

C -1.41515000 0.42310300 -0.00000600

C -1.77003500 -0.96552500 -0.00002800

C -3.10679700 -1.36193100 -0.00001700

C -4.14841500 -0.40467600 0.00002200

H 0.17568400 1.84331400 -0.00001300

H -4.58835600 1.70732600 0.00008300

C -0.07052300 0.78718400 -0.00002500

C -0.69604500 -1.91356400 -0.00006200

H -3.36044900 -2.41707600 -0.00003600

C 0.60862200 -1.52595200 -0.00007200

C 0.96384800 -0.14540400 -0.00005400

H -0.94596500 -2.96958100 -0.00008200

H 1.38635600 -2.28094600 -0.00009900

O -2.16802200 2.69738100 0.00006700

O -5.40167900 -0.76123300 0.00003500

C 2.32422600 0.32104400 -0.00006300

C 3.46019100 -0.41331600 -0.00001200

H 2.44045800 1.40258200 -0.00010900

H 3.43531800 -1.49666900 0.00006000

C 4.77447500 0.20743700 -0.00002400

C 5.95450800 -0.72261100 0.00022500

O 4.94598300 1.43277300 -0.00017500

H 6.88751900 -0.16144500 -0.00011500

H 5.91513000 -1.37142700 0.87917500

H 5.91496200 -1.37224600 -0.87810900

Resveratrone, optimized geometry in $S_0$ for $pK_a$ prediction

B3LYP/6-31+G(d)

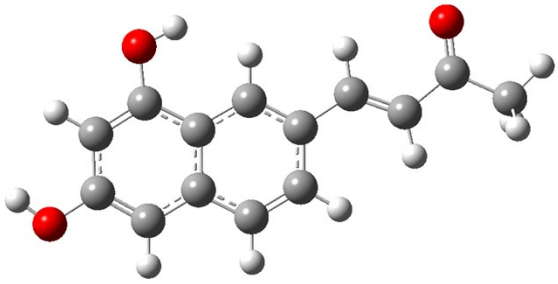

C 3.75496400 0.93903100 0.00003900

C 2.43942800 1.35979700 -0.00000800

C 1.36218500 0.41480000 -0.00002600

C 1.70290800 -0.98259100 -0.00003700

C 3.05354700 -1.39379300 0.00000000

C 4.05776700 -0.44099400 0.00004900

H -0.28805100 1.83773400 0.00004500

H 4.54822800 1.68030100 0.00005200

C -0.00238300 0.78875700 -0.00001800

C 0.63478200 -1.93141200 -0.00007900

H 3.30628300 -2.44881100 -0.00000200

C -0.67861300 -1.53750300 -0.00008800

C -1.02988200 -0.15114400 -0.00004600

H 0.88399700 -2.98872600 -0.00010100

H -1.45865400 -2.29126000 -0.00012200

O 2.23512000 2.70917400 -0.00002600

O 5.35323600 -0.87576400 0.00009400

H 1.29411100 2.92947800 -0.00023200

H 5.96448200 -0.12500800 0.00013000

C -2.40789500 0.31967700 -0.00002000

C -3.53882500 -0.42501700 0.00000200

H -2.53639400 1.40137100 -0.00001400

H -3.50702100 -1.51076200 0.00000900

C -4.87769700 0.19803500 0.00002800

C -6.05897200 -0.74841600 0.00009200

O -5.04337800 1.42304700 0.00000400

H -6.99560700 -0.18907800 0.00010300

H -6.01956700 -1.40115500 -0.88003200

H -6.01951400 -1.40110100 0.88025300

Resveratrone 1-anion, optimized geometry in $S_0$ for $pK_a$ prediction

B3LYP/6-31+G(d)

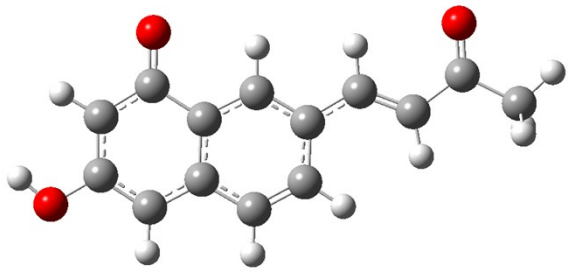

C -3.77130800 0.98958300 0.00018400

C -2.42935900 1.46698800 0.00023500

C -1.37890900 0.42978300 0.00006600

C -1.73023000 -0.96720000 -0.00014100

C -3.08072000 -1.36470500 -0.00018500

C -4.06870400 -0.37732300 -0.00001800

H 0.20731300 1.85682400 0.00027100

H -4.57792700 1.71997800 0.00030800

C -0.02645700 0.79536900 0.00011100

C -0.65913600 -1.91978000 -0.00030100

H -3.35691400 -2.41421700 -0.00034200

C 0.65696800 -1.53068900 -0.00025400

C 1.01546800 -0.14419800 -0.00004200

H -0.90934300 -2.97816600 -0.00046200

H 1.43393100 -2.28921500 -0.00037900

O -2.13582700 2.71111400 0.00041500

O -5.37541000 -0.81371000 -0.00006500

H -5.97179800 -0.05130400 0.00005900

C 2.38184200 0.32373900 0.00002100

C 3.52875000 -0.41371500 -0.00010900

H 2.50544300 1.40662000 0.00019100

H 3.50013000 -1.49994800 -0.00028000

C 4.85412500 0.20692600 -0.00001200

C 6.04160200 -0.73868500 -0.00010600

O 5.03278800 1.43640900 0.00017900

H 6.97604900 -0.17500900 -0.00055100

H 6.00882400 -1.39102100 0.88056000

H 6.00831000 -1.39162500 -0.88030100

Resveratrone 3-anion, optimized geometry in $S_0$ for $pK_a$ prediction

B3LYP/6-31+G(d)

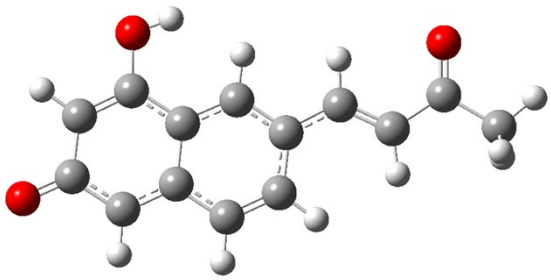

C -3.80460400 0.93119000 -0.00001300

C -2.49811000 1.34816700 -0.00002100

C -1.40672300 0.40845100 0.00000000

C -1.75985700 -0.99723600 0.00000200

C -3.09664600 -1.40576800 0.00000800

C -4.17709300 -0.47165200 0.00000400

H 0.23228400 1.83039600 0.00003200

H -4.59924900 1.67232100 -0.00003200

C -0.05318400 0.77983900 0.00001900

C -0.67507700 -1.94046200 0.00001400

H -3.33297900 -2.46737200 0.00001500

C 0.63612000 -1.54570000 0.00002100

C 0.99179400 -0.15644700 0.00002600

H -0.92025900 -2.99972000 0.00001900

H 1.41751000 -2.29931500 0.00003600

O -2.27714200 2.70682500 -0.00002800

O -5.40961600 -0.82392600 0.00000900

C 2.35427500 0.31456900 0.00003900

C 3.50377500 -0.42076800 -0.00006000

H 2.47820300 1.39751100 0.00011800

H 3.47817000 -1.50697200 -0.00016700

C 4.82585600 0.20420500 -0.00002800

C 6.01730900 -0.73656400 -0.00006500

O 5.00016700 1.43494300 0.00009200

H 6.94934500 -0.16886900 -0.00064900

H 5.98770500 -1.38889700 0.88071700

H 5.98706900 -1.38979000 -0.88015100

H -1.33208100 2.90702600 -0.00020900

Resveratrone dianion, optimized geometry in $S_0$ for $pK_a$ prediction

B3LYP/6-31+G(d)

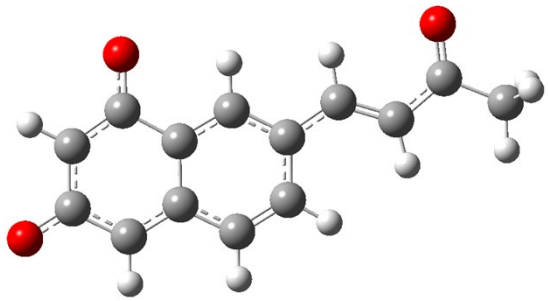

C 3.82373300 0.98262300 0.00003700

C 2.49508600 1.45950300 0.00004000

C 1.42594600 0.43046100 0.00000800

C 1.78535300 -0.97709500 -0.00002500

C 3.11942900 -1.36924100 -0.00002900

C 4.19140500 -0.40309600 0.00000300

H -0.14675200 1.85565200 0.00003600

H 4.63079100 1.71485800 0.00006000

C 0.08635400 0.79322700 0.00001100

C 0.69960800 -1.92728600 -0.00005200

H 3.37903500 -2.42631400 -0.00005400

C -0.61281000 -1.53749800 -0.00004700

C -0.97588700 -0.14594800 -0.00001600

H 0.94774800 -2.98705000 -0.00007700

H -1.39160900 -2.29507500 -0.00006800

O 2.18794100 2.71159800 0.00006800

O 5.42581200 -0.78193500 0.00000000

C -2.32317300 0.31808000 -0.00000600

C -3.49107000 -0.41838700 -0.00001500

H -2.44649700 1.40155500 0.00001100

H -3.45982000 -1.50396800 -0.00003400

C -4.79649500 0.19791900 0.00000100

C -6.01195900 -0.71990700 -0.00001300

O -4.98907300 1.43729700 0.00002900

H -6.62767300 -0.50738100 -0.88151800

H -5.74819200 -1.78056800 -0.00010400

H -6.62758400 -0.50751700 0.88158700